

RESEARCH

Open Access



Evaluating H2BC9 as a potential diagnostic and prognostic biomarker in head and neck squamous cell carcinoma

Lanhua Wu^{1,2,3,4†}, Liang Li^{5†}, Mingjing Zhu^{1,2}, Ziyang Zhou⁶, Xuejin Su⁷, Yueming Jiang^{3,4}, Min Kang^{1,2,3,4*} and Li Jiang^{1,2,3,4*}

Abstract

Background Histone H2B is highly expressed in many types of cancers and is involved in cancer development. H2B clustered histone 9 (*H2BC9*), a member of the H2B family, plays critical roles in gene expression regulation, chromosome structure, DNA repair stability, and cell cycle regulation. However, the diagnostic and prognostic value of *H2BC9* in head and neck squamous cell carcinoma (HNSCC) remains unclear. This study aimed to evaluate the potential diagnostic and prognostic value of *H2BC9* in HNSCC and investigate its biological role using bioinformatics.

Methods The expression pattern and diagnostic value of *H2BC9* in HNSCC were explored using UCSC Xena and GEO database. *H2BC9* expression was validated using the Human Protein Atlas database, qRT-PCR, and western blotting. Prognostic value was assessed using Kaplan–Meier curves, Cox regression analysis, and a nomogram. Drug sensitivity was predicted using the R package pRRophetic, and molecular interactions were analyzed using the DepMap database. The impact of *H2BC9* on HNSCC cells was further investigated through in vitro experiments.

Results *H2BC9* was markedly upregulated in HNSCC cell lines and tissues. High expression of *H2BC9* was correlated with advanced-stage disease and poor prognosis. KEGG analysis linked *H2BC9* to cell cycle regulation and DNA replication. *H2BC9* expression influenced the drug sensitivity of paclitaxel, docetaxel, cisplatin, and 5-fluorouracil. Key molecules, such as *TONSL*, *PITX2*, *NOTCH1*, and *H2BC10*, were positively correlated with *H2BC9* expression. Silencing *H2BC9* suppressed cell proliferation, induced G2/M cell cycle arrest, and enhanced apoptosis and DNA damage in HNSCC cells.

Conclusion We demonstrated that *H2BC9* expression may be associated with HNSCC development and prognosis. These findings may provide a potential therapeutic target for HNSCC.

Keywords *H2BC9*, Head and neck squamous cell carcinoma, Diagnosis, Prognosis, Drug response prediction

[†]Lanhua Wu and Liang Li have contributed equally to this work.

*Correspondence:

Min Kang

Km1019@163.com

Li Jiang

jianglixmu@163.com

Full list of author information is available at the end of the article



Introduction

Head and neck squamous cell carcinoma (HNSCC) is a diverse tumor arising from the mucosal epithelium of the oral cavity, pharynx, and larynx [1]. It is the sixth most prevalent tumor worldwide, with over 740,000 new cases and more than 360,000 deaths reported in 2020 [2]. HNSCC is characterized by a high incidence of cervical lymph node metastases, increased invasive and recurrent capabilities, and poor prognosis [1, 3, 4]. The lack of evident symptoms and reliable molecular markers for the early diagnosis of HNSCC leads to limited therapeutic effects [5]. Despite substantial progress in multidisciplinary treatments, such as surgery, radiotherapy, and chemotherapy, the 5-year overall survival (OS) of patients with HNSCC, especially those in advanced stages, remains poor [6]. Therefore, there is an urgent need to enhance prognosis by identifying new diagnostic biomarkers and therapeutic targets specific to HNSCC.

Histones, which include five types (H1, H2A, H2B, H3, and H4), bind to DNA to form chromatin in eukaryotes. The nucleosome, the basic repeating unit of chromatin, consists of two copies each of H2A, H2B, H3, and H4 [7]. H2B family genes significantly impact the prognosis of liver, lung, and breast cancers [8–10]. In gliomas, H2B plays a crucial role in the pathological process by affecting cell cycle and immune responses. Specifically, H2B clustered histone 9 (*H2BC9*) and H2B clustered histone 11 (*H2BC11*) have been identified as independent prognostic factors for glioma. Moreover, H2B mutations are particularly prevalent in certain cancer types, including HNSCC [11]. Previous studies have demonstrated a strong correlation between histone epigenetic modifications and metastasis in various cancers, including HNSCC [12]. This correlation is attributed to the alteration of signaling molecules in the epithelial-mesenchymal transformation pathway, regulated by histone post-translational modifications [13]. However, the functional role and biological mechanism of *H2BC9* in HNSCC remain unclear.

In this study, we analyzed the expression signatures, diagnostic and prognostic value, potential molecular functions, and associated pathways of *H2BC9* using multiple databases. To verify the expression of *H2BC9*, we used immunohistochemical results from the Human Protein Atlas (HPA) database, and conducted quantitative real-time PCR (qRT-PCR) and western blotting for mRNA and protein expression, respectively. Additionally, we investigated the drug sensitivity related to *H2BC9* expression and analyzed molecules associated with *H2BC9* at the cellular level. Finally, we silenced *H2BC9* expression using RNA interference to explore its molecular functions in HNSCC cell lines. The results of this study contribute to a better understanding of the role of

H2BC9 in cancer occurrence, development, and prognosis, particularly in HNSCC.

Materials and methods

Database and data acquisition

The Cancer Genome Atlas (TCGA) (<https://genomecancer.ucsc.edu/>) provides genomic, transcriptomic, and proteomic data on 33 types of cancer for >20,000 patients. Gene expression transcriptome data and clinical data were downloaded from the UCSC Xena database (<https://xenabrowser.net/datapages/>). The GSE30784 (including 167 oral squamous cell carcinoma tissues and 45 normal tissues) and GSE51985 datasets (including 10 laryngeal squamous cell carcinoma and 10 adjacent non-neoplastic tissue samples) were obtained from the GEO database (<https://www.ncbi.nlm.nih.gov/geo/>). Cancer drug sensitivity genomics data were downloaded from the Genomics of Drug Sensitivity in Cancer (GDSC) database (<https://www.cancerrxgene.org/>). Head and neck cancer cell RNAseq data were retrieved from the DepMap database (<https://depmap.org/portal/download/all/>). For chip expression profile data, probes that mapped to multiple genes were removed, for multiple probes corresponding to one gene, the maximum value was used for expression. TCGA-HNSCC expression profiles were processed using the transcripts per million (TPM) method and transformed using $\log_2(\text{TPM} + 1)$ for normalization. Immunohistochemical staining data for normal and oral squamous cell carcinoma tissues were downloaded from the HPA database (<https://www.proteinatlas.org/>). As these databases are open and accessible, approval from the local ethics committee was not required.

Analysis of *H2BC9* expression

R version 4.2.1 was used to compare the expression of the *H2BC9* gene in tumor and adjacent normal tissues, with the “ggplot2” package adopted for visualization. The GSE30784 and GSE51985 datasets were used to verify *H2BC9* expression by means of a *t* test.

Survival analysis

In TCGA-HNSCC tumor tissues, samples were divided into high- ($n=252$) and low- ($n=252$) *H2BC9* expression groups based on the median expression level of *H2BC9*. Survival probabilities were calculated using Kaplan–Meier analysis and the log-rank test. The prognostic value of *H2BC9* was further explored using the Kaplan–Meier plotter database (<http://kmplot.com/analysis>). Cox regression analysis was conducted to investigate the influence of different variables, including age, gender, grade, clinical stage, lymphnode neck dissection, primary therapy outcome, and *H2BC9* expression, on the prognosis of patients with HNSCC. Factors with $P < 0.05$ based

on univariate Cox analysis were included into the step-wise multivariate analysis. In addition, we established a nomogram based on prognostic factors to predict the OS of HNSCC. The “survival” R package was utilized for statistical analysis. The results were manifested as forest plots using the R software (Version 4.2.1) and “ggplot2” package, which displayed *P* values, hazard ratios (HRs), and their respective 95% confidence intervals (CIs). The predictive accuracy of this model was evaluated using a calibration curve. Clinical HNSCC samples from the First Affiliated Hospital of Guangxi Medical University (76 with high *H2BC9* expression vs. 76 with low *H2BC9* expression) were used to verify the prognostic value of *H2BC9* through Kaplan–Meier curve analysis.

Enrichment and gene set enrichment analysis (GSEA) analyses

Gene Ontology (GO) and Kyoto Encyclopedia of Genes and Genomes (KEGG) enrichment analyses were performed on the top 50 differentially expressed genes (DEGs), sorted by $P < 0.05$, using the “clusterProfiler 4.2.0” package [14]. GSEA of the Hallmark and KEGG gene sets was performed using the fgsea package (version 1.30.0). The enrichment strength was indicated using the normalized enrichment score (NES). The level of significance was defined at $P < 0.05$.

Drug sensitivity analysis

Sensitivity scores were used to evaluate the therapeutic response of patients with high- and low-*H2BC9* expression to candidate drugs. We utilized the R software package (pRRophetic, version 0.5) to predict the sensitivity of HNSCC samples to chemotherapy. GDSC training set was used to conduct 10-fold cross-validation tests and estimate the accuracy of IC50. By applying a filter condition of $P < 0.05$, we determined the chemotherapy sensitivity for each tumor sample.

Molecular correlation analysis at the cell line level

Data for head and neck cancer cell lines were downloaded from the DepMap database, which integrates the Cancer Cell Line Encyclopedia and Profiling Relative Inhibition Simultaneously in the Mixtures platform [15]. Data were analyzed using k-means clustering analysis or the “Data Explorer” feature in “Tools.”

Patient samples

In total, 152 pairs of HNSCC and corresponding adjacent tissues were collected from The First Affiliated Hospital of Guangxi Medical University. The recruitment phase for the study spanned from April 1, 2013 to December 31, 2018. The inclusion criteria were as follows: (1) 18–70 years old, histopathological diagnosis

of HNSCC; (2) Kanofsky performance score (KPS) ≥ 90 ; (3) underwent radical treatment according to the guidelines and (4) availability of regular follow-up information. The exclusion criteria encompassed: (1) history of any other cancer; (2) diagnosis with distant metastasis before treatment; (3) any prior treatment for HNSCC and (4) cognitive dysfunction. The studies involving human participants were reviewed and approved by the Ethics Committee of the First Affiliated Hospital of Guangxi Medical University and the approval number was 2024-E533-01. This study has been officially sanctioned by the Medical Ethics Committee of the First Affiliated Hospital of Guangxi Medical University, thereby waiving the requirement for informed consent from participants. The study did not involve minors. All experiments were performed in accordance with relevant guidelines and regulations. The study was conducted according to the Declaration of Helsinki.

Cell line and culture

The normal human nasopharyngeal epithelial (NP69), nasopharyngeal carcinoma (C666-1, 5-8F), normal keratinocyte (HaCaT), human larynx carcinoma (TU212 and Hep2), normal oral keratinocyte (NOK), and human oral squamous cell carcinoma (CAL-27) cell lines were obtained from the Nasopharyngeal Cancer Research Laboratory at Guangxi Medical University. NP69 cells were cultured in keratinocyte-SFM medium (Invitrogen, Carlsbad, CA, USA) supplemented with bovine pituitary extract (BD Biosciences, San Diego, CA, USA). Human HNSCC cells were cultured in RPMI-1640 medium (Gibco, Waltham, MA, USA) supplemented with 10% fetal bovine serum (Gibco) and 1% streptomycin (100 mg/mL)/penicillin (100 IU/mL). All cells were incubated with 5% CO₂ at 37 °C in a humidified incubator. *H2BC9*-small interfering RNAs (siRNAs, Hanbio, WuHan, China, 1×10^8 TU/mL), and the corresponding negative controls (Hanbio, 1×10^8 TU/mL) were transfected into Cal-27 and Hep2 cells using lipofectamine 3000 (Invitrogen, Carlsbad, CA, USA). The target sequences were 5′-GTTTACAAGGTGCTGAAGCAA-3′ (*siH2BC9* # 1) and 5′-TGGCTCATTACAACAAGC GTT-3′ (*siH2BC9* # 2).

qRT-PCR

Total RNA was extracted from HNSCC cells using Trizol reagent (Takara Bio, Kusatsu, Japan). The mRNA was quantitatively detected using Nano Drop (Thermo Fisher Scientific, MA, USA). cDNA was synthesized using 5× MonScript™ RTIII All-in-One Mix and dsDNase reverse transcriptase (Monad Bio, Suzhou, China). The cDNA was used for the next qPCR reaction with StepOne Plus™ RT-qPCR System (Applied Biosystems,

Sheffield Hallam University, UK). Amplification cycles consisted of pre-denaturation at 95 °C for 30 s, denaturation at 95 °C for 10 s, annealing at 55–65 °C for 10 s, and extension at 72 °C for 30 s. The cycles were carried out 40 times. The relative RNA expression was determined using the $2^{-\Delta\Delta C_t}$ method, with *GAPDH* serving as the internal control. The primer sequences used were as follows: *H2BC9*: forward: 5'-CGTTTCGACCATCACCTCCAG-3', reverse: 5'AGCCTTTGGGTTTGAACATGC-3'; and *GAPDH*: forward: 5'-AATCAAGTGGGGCGATGTG-3'; reverse: 5'-GCAAATGAGCCCCAGCCTTC-3'.

Western blotting

Total protein was extracted from cells using the RIPA reagent, protein concentration was calculated using a BCA protein assay kit (Beyotime Institute of Biotechnology, Jiangsu, China). The sample was mixed with 5× loading buffer, at a final concentration of 1×. All samples were denatured at 100 °C for 10 min. Protein samples (50 µg/well) were subjected to sodium dodecyl sulfate–polyacrylamide gel electrophoresis and then transferred onto PVDF membranes (Millipore, Billerica, MA, USA), which were blocked with 5% nonfat milk for 2 h at 37 °C. The membranes were incubated overnight at 4 °C with a primary antibody solution containing anti-*H2BC9* antibody (MA5-14835; Thermo Fisher Scientific, 1:1000) and then with a goat anti-mouse IgG(H+L) secondary antibody HRP (31430, Thermo Fisher Scientific; 1:5000) for 1 h at room temperature. Chemiluminescence detection reagents (Beyotime Biotechnology) were prepared in the dark to detect the blots.

Cell proliferation assay

Cell proliferation was assessed using the CCK-8 assay (GLPBIO). Briefly, 1×10^3 cells/well were seeded into a 96-well plate and cultured for 0, 24, 48, 72, and 96 h. CCK-8 solution (10 µL) was added to each well and incubated at 37 °C for 2 h. The optical density was measured at 450 nm using a microplate reader (Thermo Fisher Scientific). Assays were conducted with three replicates according to the manufacturer's instructions.

Apoptosis assay

Cells were plated in six-well plates at a density of 1.5×10^5 cells/well, followed by 48 h of incubation. Then, 5×10^5 cells were harvested, resuspended in 500 µL 1× binding buffer, and stained with 5 µL Annexin V-FITC and 5 µL propidium iodide (PI) using an Annexin V-FITC/PI staining kit (Keygen, Nanjing, China). Then, the cells were incubated for 15 min at room temperature in the dark. The apoptotic cells were detected using a CytoFLEX system (Beckman Coulter, Brea, CA, USA).

Cell cycle assay

Cell cycle detection was performed according to the kit's protocol (Keygen, Nanjing, China). Cal-27 and Hep2 cells were cultured in a six-well serum-free culture with 1×10^5 cells for 48 h. Then, cells were collected and adjusted to a concentration of 1×10^6 /mL. After being fixed with 70% pre-cooled ethanol at 4 °C for 3 h, the cells were stained with 500 µL PI/RNaseA working solution (PI: RNase A=9:1) at room temperature in the dark for 60 min. The number of cells in the G1, S, and G2 phases was counted using the CytoFLEX system (Beckman Coulter).

Comet assay

A comet assay was performed using the DNA Damage Detection Kit (Keygen) following the manufacturer's instructions. The cells were inoculated in a six-well plate. When the density reached 80–90%, cells were collected and diluted to 1×10^6 cells/mL. Then, cells were lysed in a specific lysis buffer (100 mM EDTA, 2.5 M sodium chloride, 10 mM Trizma base, and 1% *N*-lauroylsarcosinate, 1% Triton X-100) at 4 °C for 2 h. Next, the DNA was uncoiled and unwound in an alkaline electrophoresis buffer (1 mmol/L EDTA and 300 mmol/L NaOH) for 30 min and then used for electrophoresis. After washing the slides with 0.4 M Tris buffer, the cells were stained with a 4',6-diamidino-2-phenylindole solution for 10 min in a dark room. An Eclipse fluorescence microscope (Nikon, Tokyo, Japan) was used for the analysis. Tail moments were used to evaluate the degree of DNA damage using OpenComet v1.3.1 [16].

Statistical analysis

The expression of *H2BC9* in tumor and normal tissues was compared using the Wilcoxon rank-sum test. A paired-sample *t* test was performed to compare tumor tissues with paired adjacent normal tissues. The diagnostic values of *H2BC9* were estimated using the diagnostic receiver operating characteristic (ROC) curves and all the area under curve (AUC) values were calculated. The relationship between clinicopathological features and *H2BC9* expression was analyzed using the chi-square test. Cox regression analysis was conducted to investigate the influence of different variables on the prognosis of patients with HNSCC. For identifying risk factors impacting OS in HNSCC patients, univariate and multivariate Cox regression analyses were performed. All statistical analyses and visualizations were performed using the R software (version 4.2.1), SPSS (version 24.2; IBN, New York, USA), and GraphPad Prism (version 8.0). $P < 0.05$ was considered significantly different.

Results

Differences in *H2BC9* expression between tumor and normal tissues

The abbreviations for the 20 TCGA cancer types are shown in Additional file 1: Table S1. *H2BC9* expression was significantly upregulated in 14 of 20 tumor types in TCGA database: HNSC, LIHC, CHOL, KIRP, KIRC, LUAD, THCA, STAD, BRCA, ESCA, BLCA, CECS, LUSC, and UCEC (Fig. 1a). Further analysis of *H2BC9* and HNSCC in both TCGA-HNSCC and GEO data revealed that their expression was significantly higher in tumor tissues than that in normal tissues (Fig. 1b–d). In 43 paired samples of tumors and adjacent tissues, *H2BC9* was significantly upregulated in tumor tissues ($P < 0.0001$; Fig. 1e). ROC curve analysis demonstrated the diagnostic value of *H2BC9* in distinguishing HNSCC tissues from normal tissues (AUC=0.854, sensitivity=0.81, specificity=0.66) (Fig. 1f). This finding was corroborated by immunohistochemical results from the HPA database, showing increased *H2BC9* expression in oral squamous cell carcinoma tissues compared with that in oral mucosa tissues (Fig. 1g). qRT-PCR and western blotting indicated that the relative mRNA and protein expression levels of *H2BC9* were significantly elevated in NPC cell lines (C666-1 and 5-8F), laryngeal cancer cell lines (TU212 and Hep2), and the oral squamous cell carcinoma cell line (CAL-27) compared to normal head and neck epithelial cell line NP69 (Fig. 1h–j).

Relationship of *H2BC9* expression and clinicopathologic characteristics in HNSCC

The association between *H2BC9* mRNA expression and clinicopathological characteristics of HNSCC is presented in Table 1 and Fig. 2. High *H2BC9* expression was correlated with advanced clinical stage, T stage, N stage and tissue type (all $P < 0.05$). However, no significant differences were observed in M stage, age, gender, histologic grade, and radiation therapy (Fig. 2a–i). Furthermore, *H2BC9* expression varied by tumor type, with the lowest expression in tongue samples and the highest in mouth and throat samples (Fig. 2j).

H2BC9 as an independent prognostic indicator for HNSCC. The prognostic value of *H2BC9* in patients with HNSCC was first evaluated using the TCGA database. Kaplan–Meier analysis revealed that higher *H2BC9* expression was associated with poorer OS ($P = 0.017$) and progression-free interval (PFI) ($P = 0.048$) (Fig. 3a, b). Time-dependent ROC curves demonstrated that *H2BC9* had acceptable accuracy in predicting 1-year (AUC=0.607), 3-year (AUC=0.563), and 5-year survival rates (AUC=0.588) (Fig. 3c). Univariate and multivariate Cox regression analyses identified *H2BC9* expression (HR=1.49; 95% CI=1.04–2.14; $P = 0.0301$) and

primary therapy outcome (HR=0.2; 95% CI=0.128–0.314; $P < 0.01$) as independent prognostic indicators for HNSCC (Fig. 3d, e). To validate the prognostic value of *H2BC9*, we performed a Kaplan–Meier analysis on clinical HNSCC samples from the First Affiliated Hospital of Guangxi Medical University. Elevated *H2BC9* expression predicted a significantly poor 5-year OS ($P < 0.001$; Fig. 3f). Based on these findings, a nomogram was constructed incorporating age, primary therapy outcome, and *H2BC9* expression to predict 1-, 3-, and 5-year survival probabilities (Fig. 3g). Calibration curves demonstrated that the predicted survival closely matched the actual outcomes, indicating strong predictive capabilities of the nomogram (Fig. 3h).

Function and pathway enrichment analysis

Differential expression analysis between high- and low-*H2BC9* expression groups identified 283 DEGs, including 165 upregulated and 118 downregulated genes. The top 50 DEGs are presented in a heatmap (Fig. 4a). The GSEA of these DEGs showed significant enrichment in biological processes (BPs), cellular components (CCs), molecular functions (MFs), and various key pathways. Key BPs included regulation of mitotic nuclear division, DNA replication, and negative regulation of the immune response (Fig. 4b). Major CCs were nuclear chromosomes, spindles, and ribosomes (Fig. 4c). MFs included structural constituents of ribosomes, catalytic activity on RNA, mRNA binding, ATP-dependent activity on DNA, DNA helicase activity, and catalytic activity acting on DNA (Fig. 4d). Hallmark and KEGG pathway analyses indicated associations with E2F targets, Myc targets, G2M checkpoints, DNA repair, DNA replication, nucleotide excision repair, spliceosome, ribosome, and cell cycle pathways (Fig. 4e, f). Notably, DEGs linked to *H2BC9* were involved in critical pathways and BPs related to tumorigenesis, including the cell cycle (NES=2.28, $P < 0.01$), DNA replication (NES=2.33, $P < 0.01$), and G2M checkpoint (NES=2.69, $P < 0.01$) (Fig. 4g–i). Detailed enrichment analysis results are provided in Additional file 1: Table S2.

H2BC9 affects drug sensitivity in patients with HNSCC

To evaluate the relationship between *H2BC9* expression and drug sensitivity in patients with HNSCC, we used a sensitivity score. We found that low *H2BC9* expression significantly increased the sensitivity score for several drugs, including paclitaxel, docetaxel, cisplatin, 5-fluorouracil, gemcitabine, vinblastine, vinorelbine, AZD7762, MK-1775, tamoxifen, luminespib, Wee1 inhibitor, vincristine, AZD5438, nilotinib, and KRAS (G12C) inhibitor-12. This finding suggests that patients with low *H2BC9* expression are more sensitive to these drugs

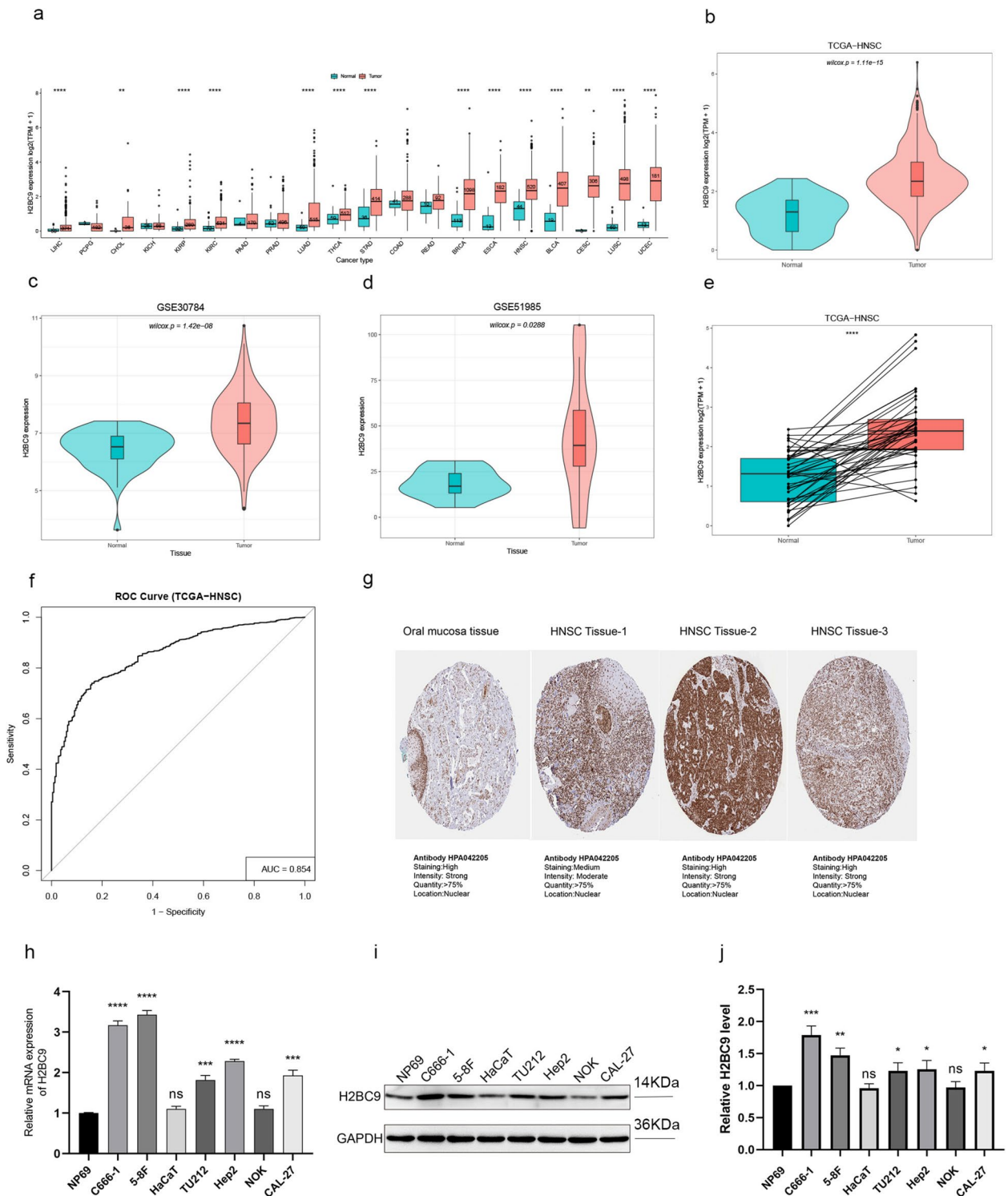


Fig. 1 *H2BC9* expression in patients with HNSCC. **a** *H2BC9* expression levels in pan-cancer from TCGA database. **b–d** The expression of *H2BC9* was significantly higher in HNSCC than that in normal tissue based on TCGA and GEO (GSE30784 and GSE51985) cohorts. **e** Expression of *H2BC9* was significantly upregulated in tumors compared with that in paired normal tissues from the TCGA database. **f** Diagnostic ROC curves show the efficiency of *H2BC9* in distinguishing tumors from non-tumor tissues. **g** The protein levels of *H2BC9* in HNSCC tissues were higher than those in normal tissues in the Human Protein Atlas. **h–j** *H2BC9* mRNA and protein expression levels were upregulated in HNSCC lines. Original blots presented in Additional file 2: Figure S1. a–d were analyzed using the Wilcoxon rank sum test, **e** was analyzed using the paired *t* test, and **h–j** were analyzed using the student's *t* tests. * $P < 0.05$, ** $P < 0.01$, *** $P < 0.001$, **** $P < 0.0001$, ^{ns} not statistically significant. HNSCC: head and neck squamous cell carcinoma

Table 1 Clinical characteristics of the patients with HNSCC based on TCGA cohort

Characteristics	Low expression of H2BC9	High expression of H2BC9	P value
<i>n</i>	252	252	
Age, <i>n</i> (%)			0.688
≤60	121 (24.1%)	126 (25%)	
>60	130 (25.8%)	126 (25%)	
Gender, <i>n</i> (%)			0.226
Female	73 (14.5%)	61 (12.1%)	
Male	179 (35.5%)	191 (37.9%)	
Clinical stage, <i>n</i> (%)			<0.001
Stage I & stage II	78 (15.9%)	37 (7.6%)	
Stage III & stage IV	169 (34.5%)	206 (42%)	
Clinical T stage, <i>n</i> (%)			<0.001
T1 & T2	112 (22.9%)	67 (13.7%)	
T3 & T4	134 (27.4%)	176 (36%)	
Clinical N stage, <i>n</i> (%)			<0.001
N0 & N1	178 (36.9%)	142 (29.5%)	
N2 & N3	64 (13.3%)	98 (20.3%)	
Clinical M stage, <i>n</i> (%)			0.974
M0	241 (50.3%)	233 (48.6%)	
M1	2 (0.4%)	3 (0.6%)	
Histologic grade, <i>n</i> (%)			0.319
G1 & G2	176 (36.4%)	187 (38.6%)	
G3 & G4	65 (13.4%)	56 (11.6%)	
Radiation therapy, <i>n</i> (%)			0.248
No	84 (19%)	71 (16.1%)	
Yes	139 (31.4%)	148 (33.5%)	
Lymphnode neck dissection, <i>n</i> (%)			0.091
No	52 (10.4%)	38 (7.6%)	
Yes	197 (39.3%)	214 (42.7%)	

H2BC9 as an independent prognostic indicator for HNSCC

(Fig. 5a–p). The remaining 62 drugs are listed in Additional file 1: Table S3. Conversely, high *H2BC9* expression significantly increased sensitivity to doramapimod, ABT737, AZD6482, and nutlin-3a (–), indicating that these patients were more sensitive to these drugs (Fig. 5q–t).

(See figure on next page.)

Fig. 2 Association between *H2BC9* expression and clinicopathologic characteristics in HNSCC from TCGA. **a** Relationship between *H2BC9* expression levels and clinicopathological features. **b** Clinical stage (stage I & stage II vs. stage III & stage IV). **c** T stage (T1 & T2 vs. T3 & T4). **d** N stage (N0 & N1 vs. N2 & N3). **e** M stage (M0 vs. M1). **f** Age (≤60 vs. >60). **g** Gender (female vs. male). **h** Histologic grade (G1 & G2 vs. G3 & G4). **i** Radiation therapy (no vs. yes). **j** *H2BC9* expression in different tissues. **a–i** were analyzed using the Wilcoxon rank sum test, **j** was analyzed using Kruskal–Wallis rank sum test. * $P < 0.05$, ** $P < 0.01$, *** $P < 0.001$, ^{ns} not statistically significant. T-tumor size status, N-lymph node status, M-metastasis, HNSCC: head and neck squamous cell carcinoma

H2BC9 and its related genes expression in HNSCC cell lines

Using data from the DepMap database, we analyzed the correlation of *H2BC9* expression with other genes in HNSCC cell lines. Key genes, such as *TONSL*, *PITX2*, *NOTCH1*, *H2BC10*, *GAL*, *CGA*, *CCS*, and *APCS*, were significantly positively correlated with *H2BC9* expression (Fig. 6).

H2BC9 affects cell proliferation, cell cycle, apoptosis, and DNA damage in vitro

Our results indicate that *H2BC9* is related to HNSCC prognosis and significantly enriched in the cell cycle pathway. Based on *H2BC9* expression in HNSCC, we selected Cal-27 and Hep2 cell lines to explore the biological function of *H2BC9*. *H2BC9* expression levels were significantly reduced after transfection with siRNA targeting *H2BC9*. As shown in Additional file 2: Figure S2. CCK-8 assay results demonstrated that the knockdown of *H2BC9* significantly reduced the proliferation of HNSCC cells (Fig. 7a, b). Additionally, suppression of *H2BC9* expression increased G2/M cell cycle arrest (Fig. 7c, d). Moreover, the downregulation of *H2BC9* significantly enhanced apoptosis and DNA damage (Fig. 7e–g).

Discussion

The escalating prevalence of HNSCC continues to pose a persistent and formidable challenge to the realm of global public health [17–19]. The high diversity and heterogeneity of HNSCC make it arduous to identify key targets to develop effective cancer therapeutics and treatment strategies [20]. Identifying new biomarkers that accurately reflect the biological characteristics of HNSCC is crucial for improving disease detection and therapy. The oncogenesis process is inherently intricate and multifaceted, encompassing a spectrum of genetic alteration, epigenetic modification, and a dysregulated tumor microenvironment [21]. Histone protein alteration or abnormal expression can drive malignant transformation [22–24]. *H2BC9* is involved in transcriptional dysregulation in cancer, cell cycle pathways, neutrophil degranulation, and interleukin signaling, all of which may play key roles in cancer progression [11]. However, the role of *H2BC9* in HNSCC has been infrequently reported.

This study provides a comprehensive analysis of the predictive value of *H2BC9* for stratifying clinicopathological

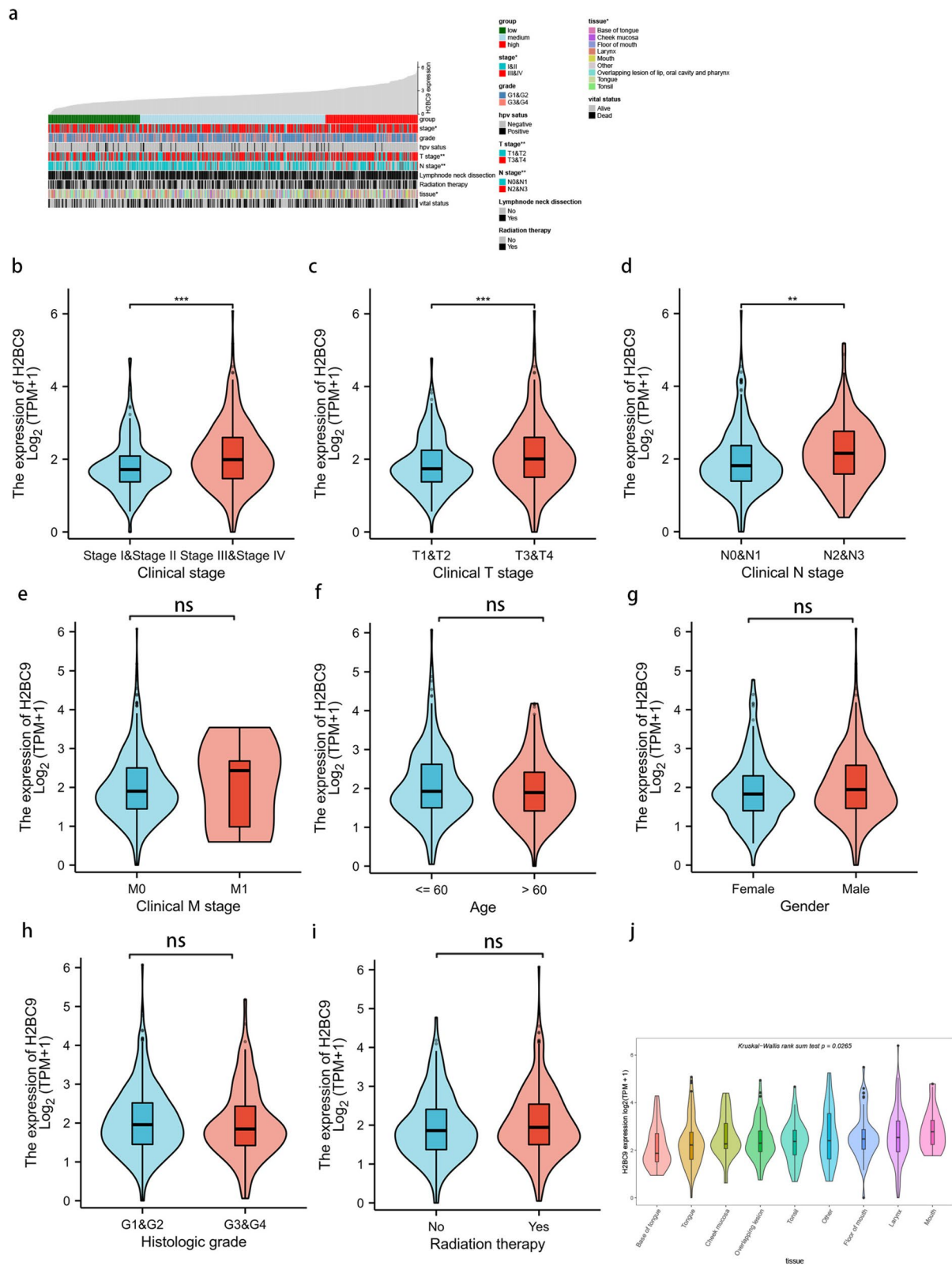


Fig. 2 (See legend on previous page.)

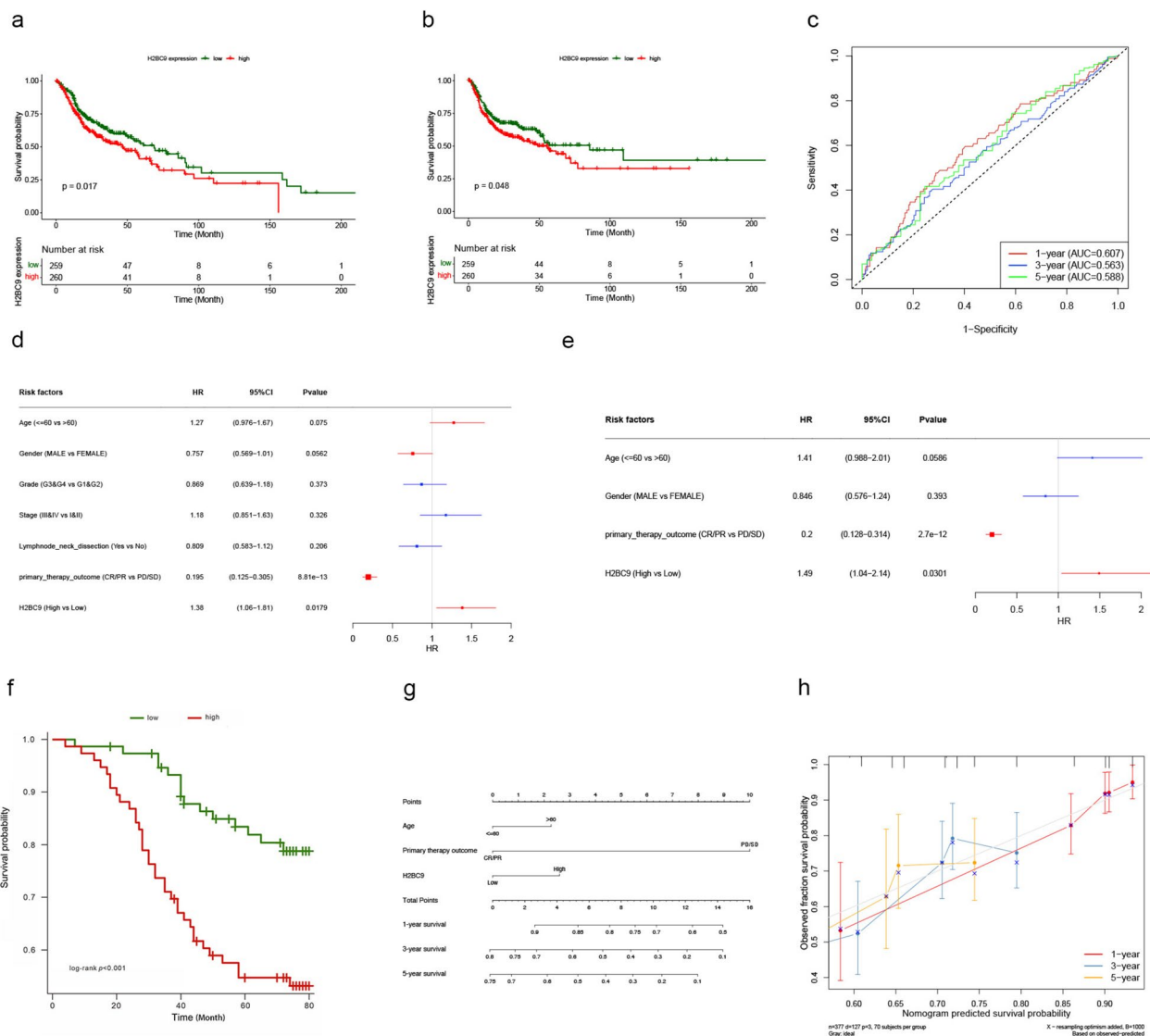


Fig. 3 Prognostic significance of *H2BC9* in HNSCC. **a,b** Kaplan–Meier curves of OS and PFI between low- and high- *H2BC9* expression in patients with HNSCC. **c** Time-dependent ROC curve of the model. **d** Univariate Cox regression analysis of *H2BC9* in HNSCC. **e** Multivariate Cox regression analysis of *H2BC9* in HNSCC. **f** 5-year OS between high- and low-*H2BC9* expression groups in clinical samples. **g** Nomogram integrating prognostic factors in HNSCC. **h** Calibration plot of the nomogram. OS: overall survival, PFI: progress-free interval, HNSCC: head and neck squamous cell carcinoma

characteristics in patients with HNSCC using a bioinformatics approach. We first utilized TCGA database to investigate *H2BC9* expression across various cancers and found that *H2BC9* was upregulated in 14 cancer types. Further analysis of TCGA and GEO databases revealed that *H2BC9* expression was significantly higher in HNSCC tissues than in normal tissues in both paired and unpaired samples. ROC curves demonstrated the diagnostic value of *H2BC9* in distinguishing patients with HNSCC from healthy individuals. Furthermore, high *H2BC9* expression correlated with T-stage, N-stage, and

overall clinical stage in HNSCC, suggesting its role in the development and progression of this cancer. qRT-PCR, western blotting, and IHC confirmed that *H2BC9* was overexpressed in HNSCC cell lines and tissues, supporting the validity of our data.

To assess the prognostic significance of *H2BC9* in patients with HNSCC, Kaplan–Meier curves were generated, showing that elevated *H2BC9* expression was associated with poorer OS and PFI. A time-dependent ROC curve confirmed the prognostic efficiency of *H2BC9* expression. Univariate and multivariate Cox regression

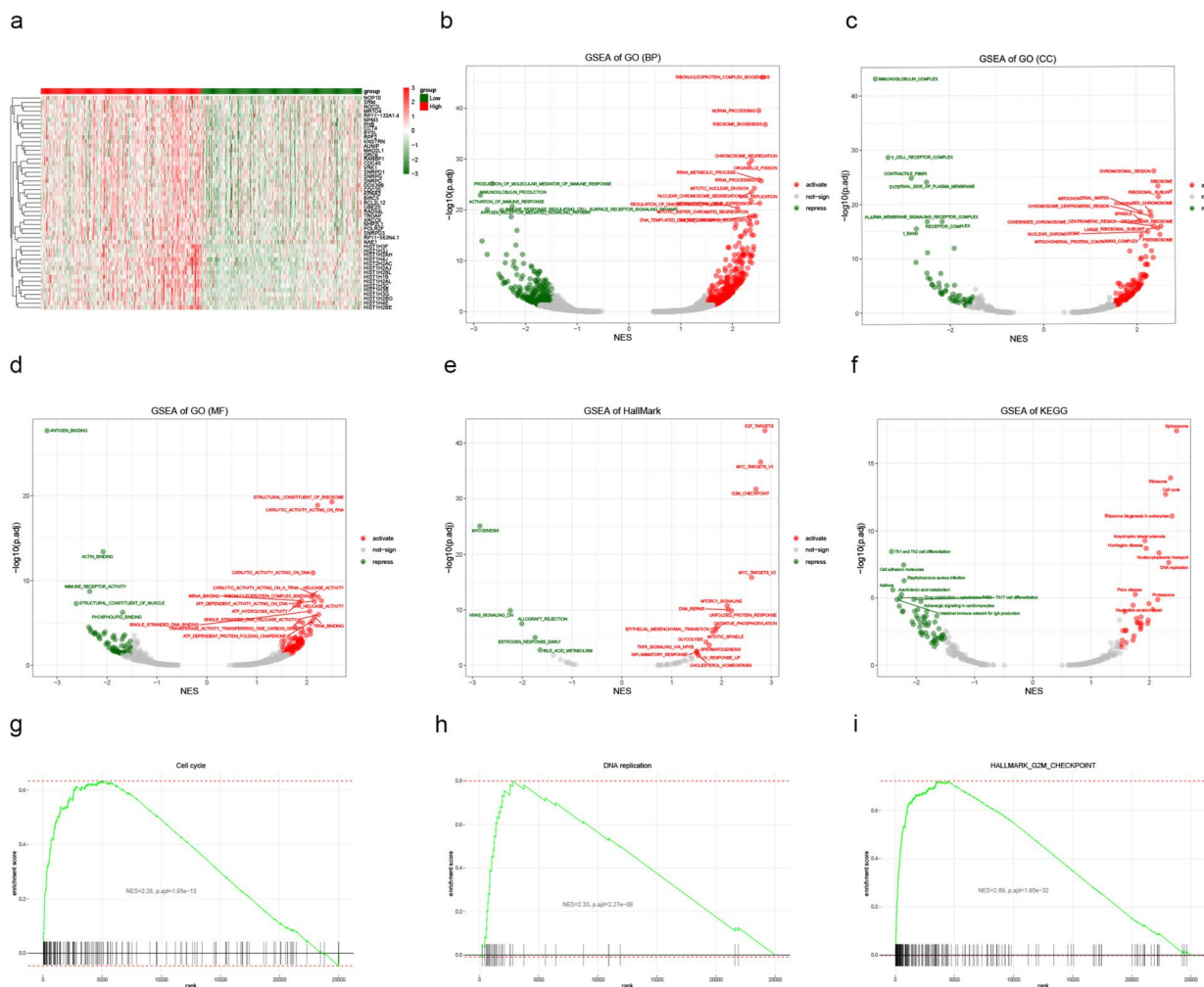


Fig. 4 Cluster analysis of *H2BC9* in TCGA HNSCC cohort. **a** Heat maps showing the correlation of the top 50 DEGs and *H2BC9* expression. **b–d** GO term enrichment analysis of DEGs. **e,f** Hallmark and KEGG enrichment analysis of DEGs. **g–i** GSEA of DEGs. DEGs: differentially expressed genes, GO: Gene Ontology, KEGG: Kyoto Encyclopedia of Genes and Genomes, GSEA: gene set enrichment analysis, TCGA: The Cancer Genome Atlas, HNSCC: head and neck squamous cell carcinoma

analyses identified primary therapy outcomes and *H2BC9* as independent prognostic indicators for patients with HNSCC. The constructed nomogram model accurately predicted the impact of age, primary therapy outcome, and *H2BC9* expression on patient survival. Previous studies have shown that *H2BC9* is an independent prognostic indicator for glioma and lung squamous cell carcinoma [9, 11]. In our study, the knockdown of *H2BC9* expression reduced HNSCC cell proliferation, increased apoptosis, and induced DNA damage by arresting the G2/M cell cycle. Overall, these results suggest that *H2BC9* is a potential diagnostic and prognostic biomarker for HNSCC.

In this study, we analyzed genes exhibiting abnormal expression patterns to understand the regulatory

networks involving *H2BC9* and the development of HNSCC. GSEA, combined with GO and KEGG enrichment analyses, revealed that *H2BC9* is associated with the G2M checkpoint, DNA repair, DNA replication, nucleotide excision repair, spliceosome, ribosome, and cell cycle pathways. Current studies on *H2BC9* in lung squamous cell carcinoma and glioma have mainly focused on its role in genetic alterations and cell cycle regulation [9, 11]. Cell cycle progression is crucial for cell proliferation and alteration and recognized as a hallmark of cancer [25, 26]. The G2/M checkpoints play an important role in cell cycle progression as they prevent DNA-damaged cells from entering mitosis [27]. In HNSCC, oncoprotein expression may cause gene mutations or inactivation, leading to a lack of Tp53

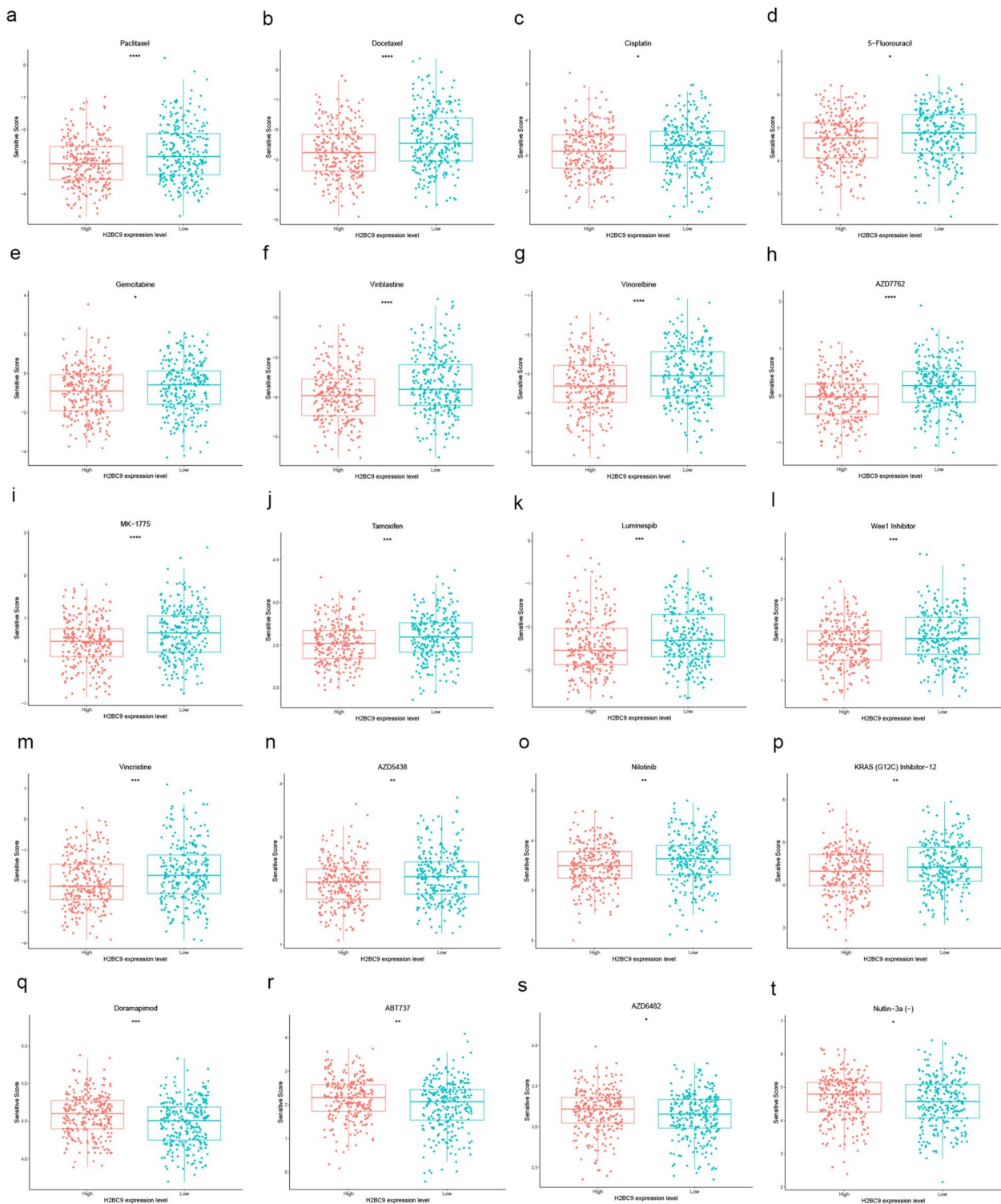


Fig. 5 Correlation between *H2BC9* and drug sensitivity in HNSCC. **a–t** Drug sensitivity of patients with HNSCC with high- vs. low- *H2BC9* expression. **a–t** were analyzed using the Wilcoxon rank sum test. * $P < 0.05$, ** $P < 0.01$, *** $P < 0.001$, **** $P < 0.0001$, HNSCC: head and neck squamous cell carcinoma

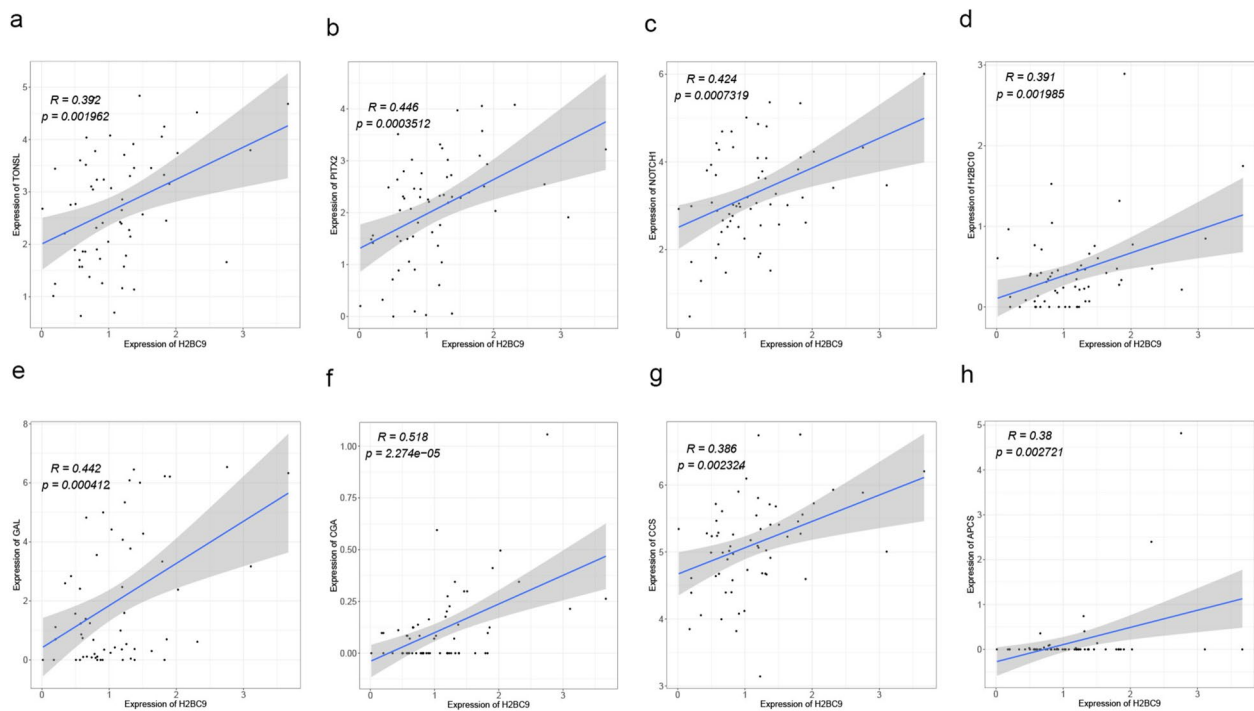


Fig. 6 Correlation between *H2BC9* and its related genes in HNSCC cell lines. **a-h** *TONSL*, *PITX2*, *NOTCH1*, *H2BC10*, *GAL*, *CGA*, *CCS*, and *APCS*. **a-h** were analyzed using Pearson's correlation analyses. HNSCC: head and neck squamous cell carcinoma

function and damage to G1/S cell cycle checkpoints, increasing the dependence on G2/M checkpoints [28–30]. Enrichment analysis indicated that the cell cycle, DNA replication, and G2/M checkpoints were significantly enriched in samples with high *H2BC9* expression, suggesting a potential mechanism involving gene mutations and cell cycle damage resulting in G2/M checkpoint activation. We hypothesize that *H2BC9* affects the cell cycle, leading to a poor prognosis of HNSCC. To confirm our hypothesis, we used *siH2BC9* in cell experiments. The results showed that inhibiting *H2BC9* expression caused cell cycle arrest in the G2/M phase while simultaneously enhancing apoptosis and DNA damage. However, further *in vivo* experiments are required to enhance the robustness of the results.

Recently, the importance of anticancer drug therapy has increased and drug therapy for HNSCC has rapidly advanced [31]. To better understand the effect of *H2BC9* on drug sensitivity in HNSCC, we performed a correlation analysis. According to the National Comprehensive Cancer Network guidelines, chemotherapeutic agents, including paclitaxel, docetaxel, cisplatin, 5-FU, and gemcitabine, are commonly used as standard chemotherapy regimens for head and neck cancer [32]. Our analysis indicated that increased *H2BC9* expression is associated with increased resistance to paclitaxel, docetaxel, carboplatin, 5-FU, cisplatin, and gemcitabine. This finding suggests that targeting

H2BC9 expression may enhance the sensitivity of patients with HNSCC to these standard chemotherapeutic agents, improving treatment outcomes. Studies have reported that paclitaxel, docetaxel, and cisplatin can induce mitotic arrest or disrupt the cell cycle, specifically interrupting the G2/M phase during mitosis [33–35]. Our enrichment analysis suggests that upregulated *H2BC9* is involved in activating G2/M checkpoints, potentially increasing DNA repair in cancer cells and allowing inappropriate proliferation [36]. The G2/M checkpoint is activated in response to endogenous DNA damage or damage induced by cancer treatments, including radiation therapy and cisplatin [37–39]. Therefore, we hypothesize that *H2BC9* enhances G2/M checkpoint activation, influencing the sensitivity to these chemotherapeutic agents. Further research *in vitro* and *in vivo* experiments are required to validate this hypothesis.

Analysis of *H2BC9* expression in HNSCC cell lines revealed that *H2BC9* positively correlates with *TONSL*, *PITX2*, *NOTCH1*, *H2BC10*, *GAL*, *CGA*, *CCS*, and *APCS*. *TONSL* knockdown in ovarian cancer increases the G2/M cell cycle proteins, cyclin B and cyclin A, and the DNA break marker protein, γ H2AX. Additionally, *TONSL* is often associated with copy number amplification (CNV) [40]. CNV is one of the most important classes of genomic mutations associated with carcinogenesis [41]. Our study found that the knockdown of *H2BC9* leads to G2/M cycle arrest and DNA damage. Based on

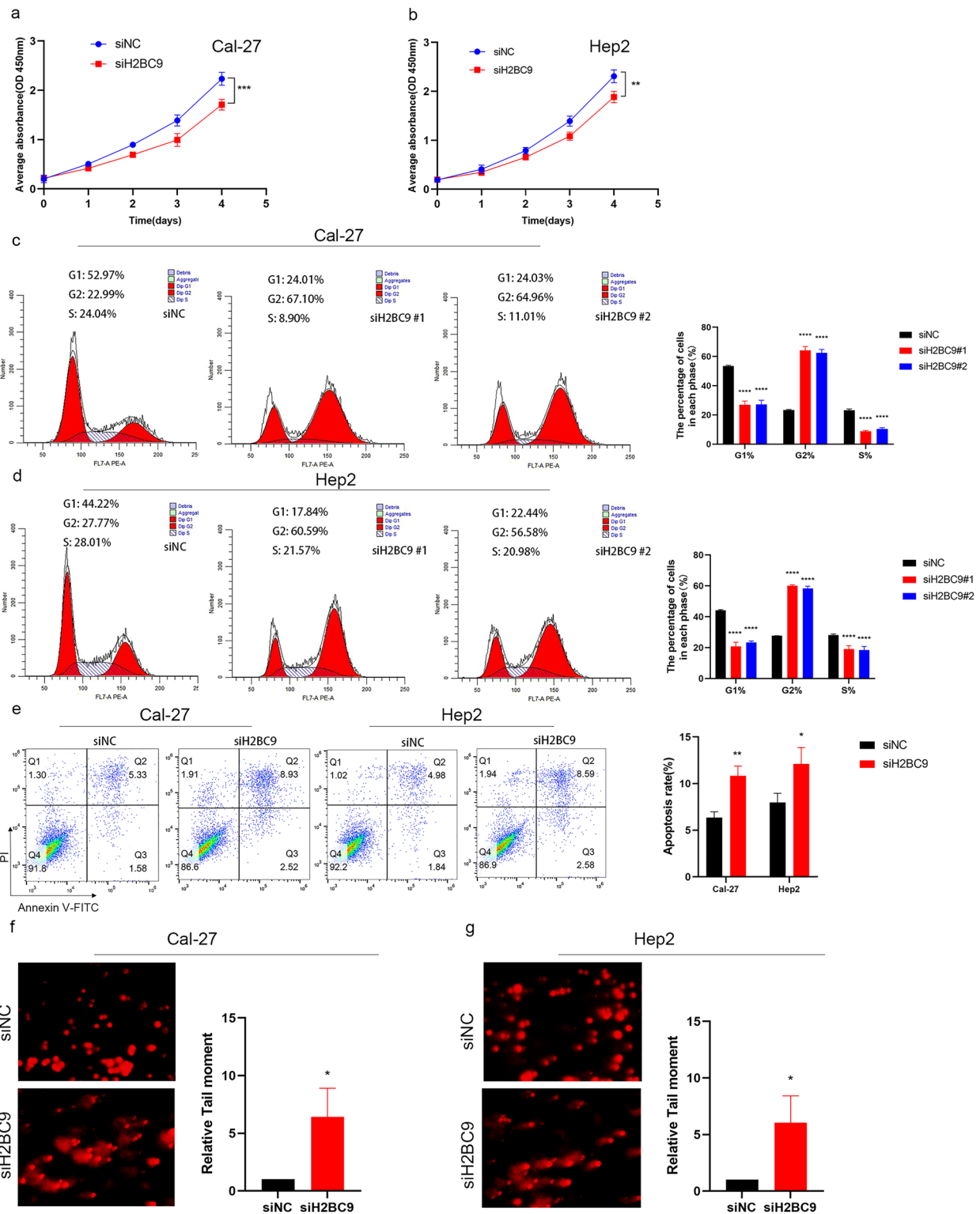


Fig. 7 Knockdown of *H2BC9* affects proliferation, cell cycle, apoptosis and DNA damage in vitro. **a,b** Knockdown of *H2BC9* suppressed the proliferation of Cal-27 and Hep2 cells. **c,d** Knockdown of *H2BC9* induced G2/M arrest of Cal-27 and Hep2 cells. **e** Knockdown of *H2BC9* induced apoptosis of Cal-27 and Hep2 cells. **f,g** Knockdown of *H2BC9* induced DNA damage of Cal-27 and Hep2 cells. Representative images of the comet assay and DNA damage in Cal-27 and Hep2 cells. Scale bars = 100 μ m. Unpaired *t* tests and one-way or two-way analysis of variance were used to determine significance. * $P < 0.05$, ** $P < 0.01$, *** $P < 0.001$, **** $P < 0.0001$

this, the intrinsic relationship between the influence of *H2BC9* on the prognosis of patients with HNSCC, and gene copy number variation and cell cycle process interference will be a novel direction for subsequent research.

DNA methylation plays an important role in the etiology, pathogenesis and prognosis of HNSCC [42]. The investigation revealed that elevated expression levels of *PITX2* correlate with suboptimal OS in HNSCC, as the hypermethylation of the *PITX2* gene suppresses its protein expression [43]. In addition, methylation of *GAL* was associated with poor survival in patients with HPV-negative oropharyngeal cancer [44]. Members of the H2B family are hypermethylated in some tumors. For example, *H2BC5*, *H2BC12*, and *H2BC18* were found to be hypermethylated in malignant pluripotent embryonic carcinoma, neuroblastomas, germ cell tumors, cervical squamous cell carcinoma, endometrial adenocarcinoma, and uterine carcinosarcoma [11]. In our study, high expression of *H2BC9* is associated with poor prognosis in HNSCC, as a member of the H2B family, the methylation status of *H2BC9* in the prognosis of HNSCC is a topic worth exploring.

NOTCH1 ranks as the second most frequently mutated gene, following closely behind TP53. Elevated *NOTCH1* expression was correlated with an unfavorable prognostic outcome in HNSCC [45, 46]. HNSCC is one of the top five cancers with H2B mutations. Our investigation has elucidated a direct correlation between the expression levels of *H2BC9* and the prognosis for patients with HNSCC, which requires further research.

The occurrence and development of tumors are intrinsically related to the changes of ubiquitin/ubiquitination (UB/UBL), which are widely involved in the control of the tumor cell cycle, apoptosis, and other biological processes [47]. In the OSCC prognostic model based on UB/UBL-related genes, *H2BC10* was one of the high-risk factors [48]. Monoubiquitination of H2B may lead to chromosomal instability phenotypes associated with mitotic chromatin compression defects, which in turn promote tumorigenesis and progression [49]. In addition, *H2BC10* is negatively correlated with CD8+ T cells, which is associated with increased pretumor immune invasion and high expression of immune checkpoints. The tumor immune microenvironment plays an important role in tumor progression, and *H2BC9* is involved in tumor immune escape [50]. In this study, we found that *H2BC9* affects the tumor cell cycle process and apoptosis. Therefore, whether this result is related to the changes of UB/UBL or the formation of immunosuppressive environment should be investigated.

Although *CGA* is rarely studied in HNSCC, the increased expression of *CGA* is involved in the

occurrence of chemotherapy resistance in patients with gastric cancer through the *CGA/EGFR/GATA2* pathway [51, 52]. Additionally, knocking out *CCS* in ovarian cancer cells increased cisplatin sensitivity. This may be mediated by the changes in SOD1 activity and ROS balance [53]. Our study found that patients with higher *H2BC9* expression exhibited higher cisplatin sensitivity compared with that of patients with lower *H2BC9* expression. However, the mechanism is still unclear. Further studies on the mechanism of *H2BC9* interactions with these chemotherapy agents will help drug therapy decision-making. *APCS*, also known as *SAP*, has been poorly studied in HNSCC, but studies have shown that the absence of SPA can promote the progression of malignant insulinoma [54]. Therefore, understanding the relationship between *H2BC9* and these genes may provide new insights into HNSCC research.

Although this research revealed some novel findings, it still has several limitations. First, the dataset employed in our investigation was predominantly sourced from a publicly accessible repository, the integrity of which is contingent upon rigorous evaluation and restricted to specific ethnic cohorts. Second, larger multi-center population cohorts were warranted to further confirm our findings. Third, in vitro and in vivo functional experiments are needed to further investigate the roles of *H2BC9* in HNSCC initiation and progression, especially in cell cycle checkpoints and drug resistance.

Conclusion

Our results indicate that *H2BC9* is a potential diagnostic and prognostic biomarker for HNSCC. *H2BC9* may influence the progression of HNSCC and contribute to therapy resistance. These findings provide a basis for further investigation into the mechanisms by which *H2BC9* affects HNSCC. Future research should focus on elucidating the specific molecular pathways regulated by *H2BC9* and its role in therapeutic resistance. Additionally, understanding the interaction of *H2BC9* with other biomarkers could lead to the development of more effective targeted therapies for HNSCC.

Abbreviations

BP	Biological process
CC	Cellular component
DEG	Differentially expressed gene
GO	Gene Ontology
GSEA	Gene set enrichment analysis
HNSCC	Head and neck squamous cell carcinoma
HPA	Human Protein Atlas
KEGG	Kyoto Encyclopedia of Genes and Genomes
MF	Molecular function
NOK	Normal oral keratinocytes
NPC	Nasopharyngeal carcinoma

OS	Overall survival
PI	Propidium iodide
PFI	Progression-free interval
qRT-PCR	Quantitative real-time PCR
TCGA	The Cancer Genome Atlas
TPM	Transcripts per million

Supplementary Information

The online version contains supplementary material available at <https://doi.org/10.1186/s40001-025-02301-3>.

Additional file 1: Table S1: Abbreviations of the 20 cancer types in The Cancer Genome Atlas database. **Table S2:** The enrichment analysis of *H2BC9* differentially ex-pressed genes. **Table S3:** Drug sensitivity of *H2BC9* in HNSCC

Additional file 2: Figure S1: Original western blotting results. **(a)** GAPDH. **(b)** *H2BC9*. **Figure S2:** Construction of HNSCC cell models with *H2BC9* knockdown. **(a, b)** qPCR were applied to examine the knockdown efficiency of *H2BC9* in Cal-27 and Hep2. Unpaired two-tailed Student's t-tests were used to determine significance. *** $P < 0.001$

Additional file 3: The raw data sources of this study

Acknowledgements

We thank Mr. Jindong Zhu (Anrenxin Biotechnology Co, Ltd at Nanning, China) for his helpful discussions and bioinformatics analysis.

Author contributions

LJ conceived and designed the project, MK designed the project and gave important suggestions to the manuscript, LHW acquired the data and written the original draft, LL analysed and interpreted the data and written the original draft, MJZ, ZYZ, XJS, and YMJ reviewed and edited draft. All the authors contributed to the manuscript and approved the submitted version.

Funding

This work was supported by grants from the National Natural Science Foundation of China (No. 82202940, 82272736, 82160467, 81460460, 81760542), The Research Foundation of the Science and Technology Department of Guangxi Province, China (grant No. 2023GXNSFDA026009, 2016GXNSFAA380252, 2018AB61001 and 2014GXNSFBA118114), the Research Foundation of the Health Department of Guangxi Province, China (No. S2018087), Guangxi Medical University Training Program for Distinguished Young Scholars (2017), Medical Excellence Award Funded by the Creative Research Development Grant from the First Affiliated Hospital of Guangxi Medical University (2016). Guangxi Medical High-level Talents Training Program, the central government guide local science and technology development projects (ZY18057006) and the Joint Project on Regional High-Incidence Diseases Research of the Guangxi Natural Science Foundation (grant no. 2023GXNSFBA026211).

Availability of data and materials

The data underlying this article will be shared on reasonable request to the corresponding author.

Declarations

Ethical approval and consent to participate

The studies involving human participants were reviewed and approved by the Ethics Committee of the First Affiliated Hospital of Guangxi Medical University and the approval number was 2024-E533-01. This study has been officially sanctioned by the Medical Ethics Committee of the First Affiliated Hospital of Guangxi Medical University, thereby waiving the requirement for informed consent from participants. The study did not involve minors. All experiments were performed in accordance with relevant guidelines and regulations. The study was conducted according to the Declaration of Helsinki.

Consent for publication

Not applicable.

Competing interests

The authors declare no competing interests.

Author details

¹Department of Radiation Oncology, The First Affiliated Hospital of Guangxi Medical University, Nanning 530021, Guangxi, China. ²Key Laboratory of Early Prevention and Treatment for Regional High Frequency Tumor (Guangxi Medical University), Ministry of Education, Nanning 530021, Guangxi, China. ³Department of Toxicology, School of Public Health, Guangxi Medical University, Nanning 530021, Guangxi, China. ⁴Guangxi Colleges and Universities Key Laboratory of Prevention and Control of Highly Prevalent Diseases, Guangxi Medical University, Nanning, China. ⁵CPC Organization and Human Resource Department, The First Affiliated Hospital of Guangxi Medical University, Nanning, 530021, Guangxi, China. ⁶Guangdong Cardiovascular Institute, Guangdong Provincial People's Hospital, Guangdong Academy of Medical Sciences, Guangzhou, Guangdong, China. ⁷Department of Oncology, Liuzhou People's Hospital Affiliated to Guangxi Medical University, Liuzhou 545006, Guangxi, China.

Received: 15 October 2024 Accepted: 15 January 2025

Published online: 27 January 2025

References

- Johnson DE, Burtneß B, Leemans CR, Lui VWY, Bauman JE, Grandis JR. Head and neck squamous cell carcinoma. *Nat Rev Dis Primers*. 2020;6(1):92.
- Sung H, Ferlay J, Siegel RL, Laversanne M, Soerjomataram I, Jemal A, et al. Global cancer statistics 2020: GLOBOCAN estimates of incidence and mortality worldwide for 36 cancers in 185 countries. *CA Cancer J Clin*. 2021;71(3):209–49.
- Chow LQM. Head and neck cancer. *N Engl J Med*. 2020;382(1):60–72.
- Duprez F, Berwouts D, De Neve W, Bonte K, Boterberg T, Deron P, et al. Distant metastases in head and neck cancer. *Head Neck*. 2017;39(9):1733–43.
- Gurbi B, Brauswetter D, Péñzes K, Varga A, Krenács T, Dános K, et al. MEK is a potential indirect target in subtypes of head and neck cancers. *Int J Mol Sci*. 2023;24(3):2782.
- Bhat GR, Hyole RG, Li J. Head and neck cancer: current challenges and future perspectives. *Adv Cancer Res*. 2021;152:67–102.
- Wan YCE, Chan KM. Histone H2B mutations in cancer. *Biomedicine*. 2021;9(6):694.
- Chai X, Guo J, Dong R, Yang X, Deng C, Wei C, et al. Quantitative acety- lome analysis reveals histone modifications that may predict prognosis in hepatitis B-related hepatocellular carcinoma. *Clin Transl Med*. 2021;11(3): e313.
- Liu X, Zhao X, Wang R, Tang X, Zhao Y, Zhong G, et al. Heterogeneous pattern of gene expression driven by TTN mutation is involved in the construction of a prognosis model of lung squamous cell carcinoma. *Front Oncol*. 2023;13: 916568.
- Wu Y, Gu Y, Guo S, Dai Q, Zhang W. Expressing status and correlation of ARID1A and histone H2B on breast cancer. *Biomed Res Int*. 2016;2016:7593787.
- Jia J, Han Z, Wang X, Zheng X, Wang S, Cui Y. H2B gene family: a prognos- tic biomarker and correlates with immune infiltration in glioma. *Front Oncol*. 2022;12: 966817.
- Wang JQ, Yan FQ, Wang LH, Yin WJ, Chang TY, Liu JP, et al. Identifica- tion of new hypoxia-regulated epithelial-mesenchymal transition marker genes labeled by H3K4 acetylation. *Genes Chromosom Cancer*. 2020;59(2):73–83.
- Markouli M, Strepkos D, Basdra EK, Papavassiliou AG, Piperi C. Prominent role of histone modifications in the regulation of tumor metastasis. *Int J Mol Sci*. 2021;22(5):2778.
- Yu G, Wang LG, Han Y, He QY. clusterProfiler: an R package for comparing biological themes among gene clusters. *OMICS*. 2012;16(5):284–7.
- Sim J, Ahn JW, Park J, Kim YJ, Jeong JY, Lee JM, et al. Non-canonical NLRP4 inflammasomes in astrocytes contribute to glioma malignancy. *Inflamm Res*. 2023;72(4):813–27.
- Estrada-Bernal A, Chatterjee M, Haque SJ, Yang L, Morgan MA, Kotian S, et al. MEK inhibitor GSK1120212-mediated radiosensitization of

- pancreatic cancer cells involves inhibition of DNA double-strand break repair pathways. *Cell Cycle*. 2015;14(23):3713–24.
17. Siegel RL, Miller KD, Fuchs HE, Jemal A. Cancer statistics, 2021. *CA Cancer J Clin*. 2021;71(1):7–33.
 18. Siegel RL, Miller KD, Fuchs HE, Jemal A. Cancer statistics, 2022. *CA Cancer J Clin*. 2022;72(1):7–33.
 19. Siegel RL, Miller KD, Wagle NS, Jemal A. Cancer statistics, 2023. *CA Cancer J Clin*. 2023;73(1):17–48.
 20. Powell SF, Vu L, Spanos WC, Pyeon D. The key differences between human papillomavirus-positive and -negative head and neck cancers: biological and clinical implications. *Cancers*. 2021;13(20):5206.
 21. Tan Y, Wang Z, Xu M, Li B, Huang Z, Qin S, et al. Oral squamous cell carcinomas: state of the field and emerging directions. *Int J Oral Sci*. 2023;15(1):44.
 22. Nacev BA, Feng L, Bagert JD, Lemiesz AE, Gao J, Soshnev AA, et al. The expanding landscape of 'oncohistone' mutations in human cancers. *Nature*. 2019;567(7749):473–8.
 23. Monteiro FL, Vitorino R, Wang J, Cardoso H, Laranjeira H, Simões J, et al. The histone H2A isoform Hist2h2ac is a novel regulator of proliferation and epithelial-mesenchymal transition in mammary epithelial and in breast cancer cells. *Cancer Lett*. 2017;396:42–52.
 24. Bhattacharya S, Reddy D, Jani V, Gadewal N, Shah S, Reddy R, et al. Histone isoform H2A1H promotes attainment of distinct physiological states by altering chromatin dynamics. *Epigenetics Chromatin*. 2017;10(1):48.
 25. Hanahan D, Weinberg RA. The hallmarks of cancer. *Cell*. 2000;100(1):57–70.
 26. Oshi M, Takahashi H, Tokumaru Y, Yan L, Rashid OM, Matsuyama R, et al. G2M cell cycle pathway score as a prognostic biomarker of metastasis in estrogen receptor (ER)-positive breast cancer. *Int J Mol Sci*. 2020;21(8):2921.
 27. Wang Y, Ji P, Liu J, Broaddus RR, Xue F, Zhang W. Centrosome-associated regulators of the G(2)/M checkpoint as targets for cancer therapy. *Mol Cancer*. 2009;8:8.
 28. Deneka AY, Einarson MB, Bennett J, Nikonova AS, Elmekawy M, Zhou Y, et al. Synthetic lethal targeting of mitotic checkpoints in HPV-negative head and neck cancer. *Cancers*. 2020;12(2):306.
 29. Hintelmann K, Berenz T, Kriegs M, Christiansen S, Gatzemeier F, Struve N, et al. Dual inhibition of PARP and the intra-S/G2 cell cycle checkpoints results in highly effective radiosensitization of HPV-positive HNSCC cells. *Front Oncol*. 2021;11: 683688.
 30. van Harten AM, Buijze M, van der Mast R, Rooimans MA, Martens-de Kemp SR, Bachas C, et al. Targeting the cell cycle in head and neck cancer by Chk1 inhibition: a novel concept of bimodal cell death. *Oncogenesis*. 2019;8(7):38.
 31. Kitamura N, Sento S, Yoshizawa Y, Sasabe E, Kudo Y, Yamamoto T. Current trends and future prospects of molecular targeted therapy in head and neck squamous cell carcinoma. *Int J Mol Sci*. 2020;22(1):240.
 32. Caudell JJ, Gillison ML, Maghami E, Spencer S, Pfister DG, Adkins D, et al. NCCN Guidelines® insights: head and neck cancers, version 1.2022. *J Natl Compr Cancer Netw*. 2022;20(3):224–34.
 33. Weaver BA. How taxol/paclitaxel kills cancer cells. *Mol Biol Cell*. 2014;25(18):2677–81.
 34. Colevas AD, Posner MR. Docetaxel in head and neck cancer: a review. *Am J Clin Oncol*. 1998;21(5):482–6.
 35. Ren M, Zhou X, Gu M, Jiao W, Yu M, Wang Y, et al. Resveratrol synergizes with cisplatin in antineoplastic effects against AGS gastric cancer cells by inducing endoplasmic reticulum stress-mediated apoptosis and G2/M phase arrest. *Oncol Rep*. 2020;44(4):1605–15.
 36. Kuntz K, O'Connell MJ. The G(2) DNA damage checkpoint: could this ancient regulator be the Achilles heel of cancer? *Cancer Biol Ther*. 2009;8(15):1433–9.
 37. Huang RX, Zhou PK. DNA damage response signaling pathways and targets for radiotherapy sensitization in cancer. *Signal Transduct Target Ther*. 2020;5(1):60.
 38. Bradbury A, Hall S, Curtin N, Drew Y. Targeting ATR as cancer therapy: a new era for synthetic lethality and synergistic combinations? *Pharmacol Ther*. 2020;207: 107450.
 39. Maréchal A, Zou L. DNA damage sensing by the ATM and ATR kinases. *Cold Spring Harb Perspect Biol*. 2013;5(9): a012716.
 40. Lee H, Ha S, Choi S, Do S, Yoon S, Kim YK, et al. Oncogenic impact of TONSL, a homologous recombination repair protein at the replication fork, in cancer stem cells. *Int J Mol Sci*. 2023;24(11):9530.
 41. Gao B, Baudis M. Signatures of discriminative copy number aberrations in 31 cancer subtypes. *Front Genet*. 2021;12: 654887.
 42. Zhou C, Ye M, Ni S, Li Q, Ye D, Li J, et al. DNA methylation biomarkers for head and neck squamous cell carcinoma. *Epigenetics*. 2018;13(4):398–409.
 43. Zhao Y, Zhao J, Zhong M, Zhang Q, Yan F, Feng Y, et al. The expression and methylation of PITX genes is associated with the prognosis of head and neck squamous cell carcinoma. *Front Genet*. 2022;13: 982241.
 44. Misawa K, Mochizuki D, Endo S, Mima M, Misawa Y, Imai A, et al. Site-specific methylation patterns of the GAL and GALR1/2 genes in head and neck cancer: potential utility as biomarkers for prognosis. *Mol Carcinog*. 2017;56(3):1107–16.
 45. Fukusumi T, Califano JA. The NOTCH pathway in head and neck squamous cell carcinoma. *J Dent Res*. 2018;97(6):645–53.
 46. Schmidl B, Siegl M, Boxberg M, Stögbauer F, Jira D, Winter C, et al. NOTCH1 intracellular domain and the tumor microenvironment as prognostic markers in HNSCC. *Cancers*. 2022;14(4):1080.
 47. Zhou L, Jiang Y, Luo Q, Li L, Jia L. Neddylation: a novel modulator of the tumor microenvironment. *Mol Cancer*. 2019;18(1):77.
 48. Deng SZ, Wu X, Kong L, Cheng B, Dai L. Ubiquitination, SUMOylation, and NEDDylation related genes serve as prognostic and therapeutic biomarkers for oral squamous cell carcinoma. *J Oral Pathol Med*. 2024;53(2):114–23.
 49. Jeusset LM, Guppy BJ, Lichtensztejn Z, McDonald D, McManus KJ. Reduced USP22 expression impairs mitotic removal of H2B monoubiquitination, alters chromatin compaction and induces chromosome instability that may promote oncogenesis. *Cancers*. 2021;13(5):1043.
 50. Berger KN, Pu JJ. PD-1 pathway and its clinical application: a 20 year journey after discovery of the complete human PD-1 gene. *Gene*. 2018;638:20–5.
 51. Cao T, Lu Y, Wang Q, Qin H, Li H, Guo H, et al. A CGA/EGFR/GATA2 positive feedback circuit confers chemoresistance in gastric cancer. *J Clin Invest*. 2022;132(6): e154074.
 52. Wang P, Zhou Y, Wang J, Zhou Y, Zhang X, Liu Y, et al. miR-107 reverses the multidrug resistance of gastric cancer by targeting the CGA/EGFR/GATA2 positive feedback circuit. *J Biol Chem*. 2024;300(8): 107522.
 53. Bompiani KM, Tsai CY, Achatz FP, Liebig JK, Howell SB. Copper transporters and chaperones CTR1, CTR2, ATOX1, and CCS as determinants of cisplatin sensitivity. *Metallomics*. 2016;8(9):951–62.
 54. Jiang G, Xu S, Mai X, Tu J, Wang L, Wang L, et al. SAP deletion promotes malignant insulinoma progression by inducing CXCL12 secretion from CAFs via the CXCR4/p38/ERK signalling pathway. *J Cell Mol Med*. 2024;28(10): e18397.

Publisher's Note

Springer Nature remains neutral with regard to jurisdictional claims in published maps and institutional affiliations.